

PHYSICS CONTRIBUTION

VARIABLE CIRCULAR COLLIMATOR IN ROBOTIC RADIOSURGERY: A TIME-EFFICIENT ALTERNATIVE TO A MINI-MULTILEAF COLLIMATOR?

STEVEN VAN DE WATER, M.Sc.,* MISCHA S. HOOGEMAN, Ph.D.,* SEBASTIAAN BREEDVELD, M.Sc.,*
JOOST J. M. E. NUYTENS, M.D., Ph.D.,* DENNIS R. SCHAART, Ph.D.,† AND BEN J. M. HEIJMEN, Ph.D.*

*Department of Radiation Oncology, Erasmus Medical Center–Daniel den Hoed Cancer Center, Rotterdam, The Netherlands;

†Department of Radiation Detection and Medical Imaging, Delft University of Technology, Delft, The Netherlands

Purpose: Compared with many small circular beams used in CyberKnife treatments, beam's eye view-shaped fields are generally more time-efficient for dose delivery. However, beam's eye view-shaping devices, such as a mini-multileaf collimator (mMLC), are not presently available for CyberKnife, although a variable-aperture collimator (Iris, 12 field diameters; 5–60 mm) is available. We investigated whether the Iris can mimic noncoplanar mMLC treatments using a limited set of principal beam orientations (nodes) to produce time-efficient treatment plans.

Methods and Materials: The data from 10 lung cancer patients and the beam-orientation optimization algorithm "Cycle" were used to generate stereotactic treatment plans (3×20 Gy) for a CyberKnife virtually equipped with a mMLC. Typically, 10–16 favorable beam orientations were selected from 117 available robot node positions using beam's eye view-shaped fields with uniform fluence. Second, intensity-modulated Iris plans were generated by inverse optimization of nonisocentric circular candidate beams targeted from the same nodes selected in the mMLC plans. The plans were evaluated using the mean lung dose, lung volume receiving ≥ 20 Gy, conformality index, number of nodes, beams, and monitor units, and estimated treatment time.

Results: The mMLC plans contained an average of 12 nodes and 11,690 monitor units. For a comparable mean lung dose, the Iris plans contained 12 nodes, 64 beams, and 21,990 monitor units. The estimated fraction duration was 12.2 min (range, 10.8–13.5) for the mMLC plans and 18.4 min (range, 12.9–28.5) for the Iris plans. In contrast to the mMLC plans, the treatment time for the Iris plans increased with an increasing target volume. The Iris plans were, on average, 40% longer than the corresponding mMLC plans for small targets (<80 cm³) and $\leq 121\%$ longer for larger targets. For a comparable conformality index, similar results were obtained.

Conclusion: For stereotactic lung irradiation, time-efficient and high-quality plans were obtained for robotic-controlled noncoplanar treatments using a mMLC. Iris is a time-efficient alternative for small targets, with similar or better plan quality. © 2011 Elsevier Inc.

Variable-aperture collimator, Noncoplanar beam orientation optimization, Inverse optimization, Stereotactic radiotherapy, Lung.

INTRODUCTION

Excellent local tumor control has been achieved in patients with early-stage non–small-cell lung cancer treated using the CyberKnife Robotic Radiosurgery System (Accuray, Sunnyvale, CA). The CyberKnife consists of a compact 6-MV linear accelerator mounted on a robotic manipulator and performs real-time tumor tracking to compensate for respiratory motion. Despite the high local tumor control rates, the long treatment time per fraction is an area for improvement (1).

The fraction duration mainly consists of the beam-on time, robot motion time, and image guidance time and can be reduced by developing time-efficient treatment plans.

The beam-on time can be reduced by reducing the number of monitor units (MUs). The robot motion time—the prevalent factor—can be reduced by reducing the number of node positions and beams. The node positions are the preset locations where the robotic manipulator can position the focal spot of the linear accelerator (*i.e.*, the source of the X-ray beam). From these node positions, multiple beams can be targeted at various locations in the tumor by adjusting the orientation of the linear accelerator. Traveling between node positions takes longer than a reorientation of the linear accelerator between beams at a node position. The imaging time is reduced automatically by reducing the overall

Reprint requests to: Steven van de Water, M.Sc., Department of Radiation Oncology, Erasmus Medical Center–Daniel den Hoed Cancer Center, Groene Hilledijk 301, Rotterdam 3075 EA The Netherlands. Tel: (+311) 0704-1111; Fax: (+311) 0704-1012; E-mail: s.vandewater@erasmusmc.nl

Presented in part at the 51st Annual Meeting of the American Society for Radiation Oncology, Chicago, November 2009.

Conflict of interest: none.

Acknowledgments—The authors would like to thank Warren Kilby for his contribution to our treatment time estimator and general discussions.

Received June 7, 2010, and in revised form Nov 3, 2010. Accepted for publication Dec 6, 2010.

treatment time, because fewer images are required to ensure position and tracking accuracy.

The number of node positions, beams, and MUs in a treatment plan can be reduced by increasing the degrees of freedom of beam collimation. The CyberKnife at our institute has 12 collimators with fixed circular apertures ranging from 5 to 60 mm in diameter. Generally, only one or two collimators are used per treatment. Clinical treatment plans typically contain 60 node positions, 125 beams, and 35,000 MUs. Pöll *et al.* (1) showed that the number of MUs in lung cancer treatments could be reduced by an average of 31% if two collimator sizes were used instead of one. An even larger reduction in the required number of MUs (~60% in lung cancer treatments) was achieved when a variable-aperture collimator was used (2). This variable-aperture collimator is called the Iris Variable Aperture Collimator (Accuray) and allows 12 field diameters to be used without the manual exchange of collimators.

A mini-multileaf collimator (mMLC) mounted on the CyberKnife could lead to even more time-efficient treatment plans, because it does not restrict the field to a circular field shape as does the Iris collimator. It allows for three-dimensional conformal radiotherapy (3D-CRT) to be performed using fields shaped according to the beam's eye view projection of the target. This will make dose painting with a large number of circular beams superfluous, thereby reducing the required number of beams and MUs. Moreover, a mMLC is also expected to require a limited set of node positions, because a feasible number of beam directions is 10–15 in stereotactic radiotherapy for lung and liver lesions using a MLC (3, 4). A CyberKnife equipped with a mMLC could even be more efficient in delivering noncoplanar beams than gantry-based modalities, because time-consuming manual couch adjustments would not be required. However, a mMLC is not yet available for the CyberKnife.

The goal of the present study was first to assess the plan quality and delivery time for computer-optimized noncoplanar 3D-CRT plans designed for a CyberKnife theoretically equipped with a mMLC. The second goal was to compare these mMLC plans with intensity-modulated plans developed for the currently available Iris collimator, only using those node positions selected in the mMLC plans to generate time-efficient treatment plans. To generate the Iris plans, a dedicated inverse planning algorithm was developed in-house for the present study.

METHODS AND MATERIALS

Patient group and dose prescriptions

The data from 10 lung cancer patients treated at our clinic with the CyberKnife were used. These patients were also included in the study by Pöll *et al.* (1). The gross target volume ranged from 5.9 to 78.0 cm³ (median, 14.1) and was delineated using the lung level and window settings on computed tomography (CT). A gross target volume to planning target volume (PTV) margin of 5 mm was used to include microscopic extension of the tumor and to account for inaccuracies of the Synchrony Respiratory Tracking System (5). The PTV ranged from 20.8 to 152.3 cm³ (median, 40.5).

The PTV was prescribed a dose of 60 Gy at an isodose level of $\geq 80\%$, to be delivered in three fractions. At least 95% of the PTV had to receive ≥ 60 Gy. The dose constraints for the organs at risk were mainly defined by the Radiation Therapy Oncology Group 0236 protocol for stereotactic radiotherapy for lung cancer (6). These constraints are listed in Table 1. A conformity index (CI) of ≤ 1.20 was required, defined as the ratio of the volume receiving the prescription dose (≥ 60 Gy) and the PTV.

CyberKnife characteristics

One of the standard CyberKnife extracranial node sets was used, which included 117 node positions. The node positions are distributed semispherically (noncoplanar) around the patient at a distance to the imaging center of 800–1000 mm. Each node position effectively acts as a focal spot position. The Iris variable aperture collimator allows 12 field diameters to be used: 5, 7.5, 10, 12.5, 15, 20, 25, 30, 35, 40, 50, and 60 mm defined at 800 mm from the focal spot (2). The 6-MV linear accelerator delivers an unflattened beam and is calibrated such that 1 MU corresponds to a dose of 1 cGy in a reference point located on the central axis of a 60-mm field, at 800 mm from the focal spot and a 15 mm depth in water.

Step 1: mMLC plans generated using “Cycle”

The mMLC plans for the CyberKnife were developed using Cycle, an algorithm developed in-house for simultaneous optimization of beam orientations, shapes, and weights (7). Cycle generates treatment plans by sequential selection of beams from a set of user-defined candidate beam orientations. Sequential selection means that the planning process starts with an empty plan and that beams are added one by one to the plan. In each iteration, the optimal beam is selected from the candidate beam orientations using a weighted-sum score function, which takes into account the imposed dose constraints and the dose given by the beams previously added to the plan. Favorable beam orientations can be selected more than once, increasing the beam weight. The iterations are performed until a feasible solution has been found (*i.e.*, a solution that satisfies all dose constraints). The minimization or maximization of plan parameters can be achieved by repetitive application of Cycle, each time adjusting the constraint until a feasible solution can no longer be found.

In the present study, the candidate beam orientations were defined by the 117 node positions of the CyberKnife and the center of mass of the tumor as the isocenter. The 3D-CRT fields were shaped, assuming the use of a mMLC with a resolution of 2.5 mm at the

Table 1. Maximal dose constraints for organs at risk and conformity constraint

Organ	Volume	Dose
Spinal cord	Any point	6 Gy/fraction
Liver	Any point	8 Gy/fraction
Ipsilateral brachial plexus	Any point	8 Gy/fraction
Esophagus	Any point	9 Gy/fraction
Heart	Any point	10 Gy/fraction
Trachea and main bronchus	Any point	10 Gy/fraction
Ribs	Any point	20 Gy/fraction
Lung	<10% of total volume	20 Gy in total
Conformality constraint	<1.2 * PTV	60 Gy in total

Abbreviation: PTV = planning target volume.

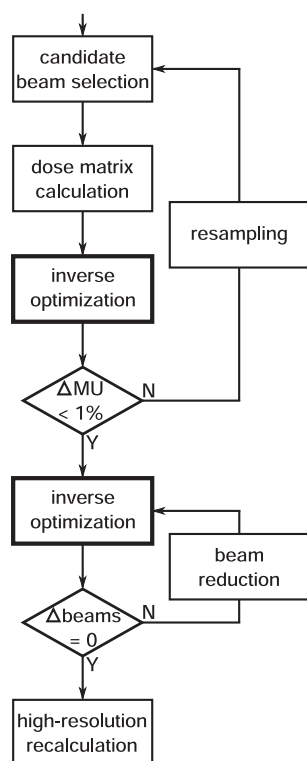


Fig. 1. Flow chart of inverse planning algorithm for Iris plans.

isocenter. The beam's eye view projection of the PTV was taken as the initial field shape for each beam. This field shape was subsequently optimized by extending or retracting the edges of the field in four perpendicular lateral directions, according to de Pooter *et al.* (8). Performing 3D-CRT requires the CyberKnife to be additionally equipped with a flattening filter. Because such a CyberKnife does not exist, the beam data from a gantry-based 6-MV linear accelerator equipped with a mMLC and flattening filter was used, normalized according to the CyberKnife conventions. The field intensity was uniform, and the penumbra was constructed by convolution of the field intensity matrix with an off-axis kernel. The dose was calculated on a rectangular dose grid with a grid spacing of $3 \times 3 \times 3$ mm or $3 \times 3 \times 2$ mm, depending on the CT slice spacing. An equivalent path-length algorithm was used to correct for density heterogeneities. After obtaining the final treatment plan, the dose was recalculated using a grid spacing of $1 \times 1 \times 1.5$ mm or $1 \times 1 \times 2$ mm, depending on the CT slice spacing.

Step 2: Iris plans generated using inverse optimization

The treatment plans for the Iris collimator (Iris plans) were generated using a new treatment planning algorithm for the CyberKnife that has been developed in-house for the present study. A flow chart of the planning algorithm is depicted in Fig. 1.

The planning process starts with the selection of candidate beams, defined by a node position, a target point, and a collimator size. For each node position, a projection of the PTV was made onto a reference plane at 800 mm from the node position. The target points were regularly distributed over the reference plane with user-defined spacing. For all target points within the projected PTV contour, all 12 collimator sizes were selected as candidate beams. The target point spacing was set to 7–14 mm, depending on the tumor size and number of node positions, to obtain 3,000–4,000 candidate beams. For each patient, only those node positions selected by Cycle in the mMLC plan were used for candidate beam selection.

The next step is the construction of an individual dose matrix for each structure involved in the optimization, containing the dose deposited (in Gy/MU) in every voxel of the structure by every candidate beam. It was constructed by performing dose calculations for each element of the matrix, using the tissue maximal ratio/off-axis ratio formalism and beam data from the CyberKnife. Density heterogeneities were accounted for by calculating the equivalent path length for each voxel. The use of separate dose matrices for each structure allowed the dose grid spacing to be adjusted to the size of the structure. The default grid spacing was set to $3 \times 3 \times 3$ mm or $3 \times 3 \times 2$ mm, depending on the CT slice spacing. Smaller grid spacing was used to ensure sufficient coverage or sparing of small structures. Larger grid spacing was used for large structures such as the lung. The final dose distribution in the entire patient was recalculated using a dose grid spacing of $1 \times 1 \times 1.5$ mm or $1 \times 1 \times 2$ mm, depending on the CT slice spacing.

The core of the planning algorithm is the inverse multicriteria optimization algorithm developed in-house by Breedveld *et al.* (9). Using dose matrices and prescriptions as input, it is capable of determining the optimal weights (in MU) of the candidate beams. It makes a distinction in the prescriptions between the constraints and objectives. The constraints are prescriptions that must be fulfilled, otherwise the solution is invalid. Objectives are prescriptions for which the optimal value (minimum or maximum) is searched without violating the constraints. Minimization of the total number of MUs was the only objective in the optimization of the Iris plans. Because the linearity of the dose delivery cannot be guaranteed at <5 MU/fraction, the candidate beams should either be ascribed ≥ 15 MU (in three fractions) or not selected at all. This

Table 2. Average plan parameters of mMLC plans, MLD-equivalent Iris, CI-equivalent Iris plans, and preferred Iris plans

Parameter	mMLC	MLD-equivalent Iris	CI-equivalent iris	Preferred iris
MLD (Gy)	8.0 (4.8–12.3)	7.8 (4.3–12.3)*	7.9 (4.0–12.2)	7.4 (4.0–11.4)*
V ₂₀ (%)	3.9 (2.4–6.7)	3.8 (2.1–6.4)	3.9 (2.0–6.4)	3.6 (2.0–6.0)*
CI	1.20 (1.14–1.27)	1.17 (1.11–1.20)	1.17 (1.11–1.20)	1.15 (1.09–1.20)
Node positions (n)	12.4 (10–16)	11.7 (10–14)	11.8 (10–15)	11.5 (9–14)*
Beams (n)	12.4 (10–16)	63.5 (31–120)*	59.2 (34–120)*	59.6 (31–127)*
MUs (n)	11,690 (10,764–13,554)	21,990 (14,692–33,358)*	21,215 (14,692–31,217)*	21,961 (16,695–32,849)*
Fraction duration (min)	12.2 (10.8–13.5)	18.4 (12.9–28.5)*	17.8 (12.9–28.5)*	18.1 (14.0–29.8)*

Abbreviations: mMLC = mini-multileaf collimator; MLD = biologically equivalent mean lung dose of 2 Gy fractions; V₂₀ = percentage of total lung volume receiving ≥ 20 Gy; CI = conformality index (ratio of volume receiving prescription dose ≥ 60 Gy] and PTV); MU = monitor unit; PTV = planning target volume.

* Significantly different ($p < .05$) from mMLC plans (Wilcoxon signed-rank test).

was achieved by repeating the inverse optimization, typically one to three times, each time excluding the beams that had been ascribed ≤ 15 MU, until all remaining candidate beams had a weight of ≥ 15 MU. Typically, only a small fraction of the candidate beams (~ 60 – 360 beams) was not excluded. Because the CI constraint could not be directly included in the optimization, a maximal dose constraint on a shell structure around the PTV was used as a surrogate.

As can be seen in Fig. 1, the steps described are embedded in the so-called resampling loop. Resampling is a method to improve the optimality of a treatment plan by iteratively increasing the total number of candidate beams (10). It makes use of the fact that most of the candidate beams are excluded by the inverse optimization, owing to the minimal beam weight of 15 MU. In each resampling run, all excluded candidate beams were replaced by newly selected candidate beams, after which the inverse optimization was repeated. The new candidate beams were selected by repeating the candidate beam selection using a target point spacing lowered by 1 mm. A decreasing target point spacing results in an increasing number of candidate beams and resampling was terminated when the maximum of 10,000 candidate beams was exceeded. Resampling was also terminated when the improvement in the number of MUs was $< 1\%$.

The final optimization step is the minimization of the total number of beams in the treatment plan, indicated by the beam reduction loop in Fig. 1. During beam reduction, the inverse optimization was performed repeatedly, each time excluding beams with the lowest contribution, until a feasible solution could no longer be found. The contribution of a beam was defined as the dose delivered to the isocenter, if the beam would have been targeted at the isocenter.

Plan evaluation

All treatment plans were inspected by a physician and only clinically acceptable plans were included. The quality of the treatment plans was assessed using the biologic equivalent mean lung dose of 2 Gy fractions (MLD), total lung volume receiving ≥ 20 Gy, CI, number of node positions, number of beams, total number of MUs, and estimated treatment time for each fraction. The MLD is the most accurate parameter to predict the incidence of radiation pneumonitis and was calculated using the linear quadratic model ($\alpha/\beta = 3$ Gy for the lung) (11). The estimated treatment time for each fraction was calculated using a dedicated algorithm that included the beam-on time, robot motion time, and time needed for imaging during treatment. It assumed a dose rate of 800 MU/min, a CyberKnife G4 robot speed, and approximately 5 s/image pair, acquired every three beams. Because the CyberKnife is not equipped with a flattening filter, the beam-on time of the mMLC plans was increased by 20% to account for flattening of the fields, according to the off-axis profile of the uncollimated CyberKnife beam. The treatment time estimations did not include the time needed for patient setup or for building a correlation model between the positions of the implanted markers and external markers on the patient's chest (5).

The MLD was used as primary objective in the comparison of the mMLC and Iris plans. For each patient, the MLD was minimized in the mMLC plan and an equal MLD was aimed at in the MLD-equivalent Iris plan. In addition, several Iris plans with varying MLD constraints were developed for each patient. A relaxed MLD constraint (15 Gy) was described for the first plan and was lowered by 0.5 Gy in successive Iris plans until a feasible treatment plan could no longer be found, thereby, resulting in the range of MLD values that can be obtained within other constraints. From all Iris plans, a CI-equivalent Iris plan was selected, having a CI

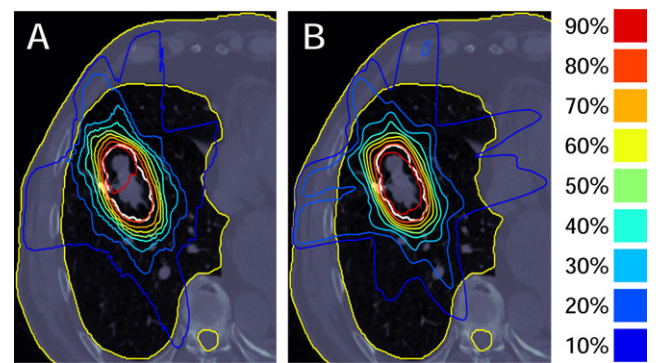


Fig. 2. Dose distributions of (A) mini-multileaf collimator plan and (B) mean lung dose-equivalent Iris plan for Patient 4 (isocenter slice). Thick white lines indicate planning target volume contour. Depicted isodose lines ranged from 10% to 90% of maximal planning target volume dose.

closest to that of the mMLC plan. Finally, the physician selected the one preferred Iris plan from all Iris plans for each patient that in the physician's opinion provided the optimal balance between the plan quality and treatment time.

RESULTS

Table 2 lists the average plan parameters for the mMLC plans, the MLD-equivalent Iris plans, the CI-equivalent Iris plans, and the preferred Iris plans. Cycle selected 10–16 node positions in the mMLC plans, depending on the patient. These node positions were subsequently used in the generation of the Iris plans. The average estimated treatment time/fraction was 12.2 min for the mMLC plans and 18.4 min for the MLD-equivalent Iris plans. When the CI was used as similarity measure, the results differed little

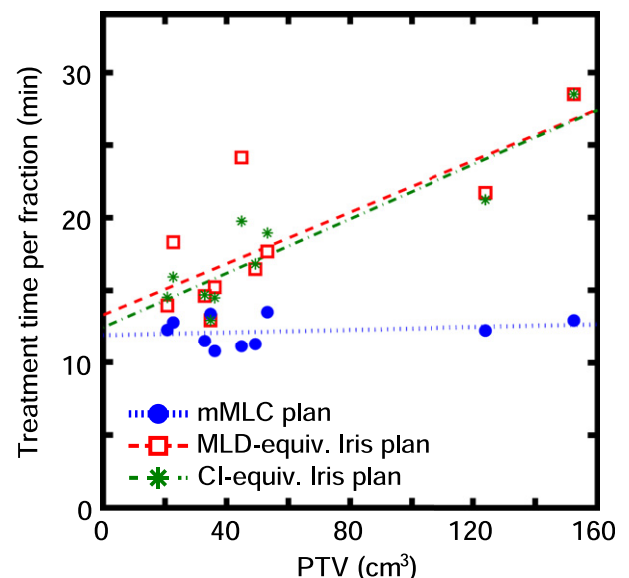


Fig. 3. Estimated treatment time/fraction as function of planning target volume for all 10 patients. Lines indicate linear fits to data (mini-multileaf collimator, $R^2 = 0.04$, $p = .6$; mean lung dose-equivalent Iris, $R^2 = 0.62$, $p = .007$; conformity index-equivalent Iris, $R^2 = 0.81$, $p < .001$; t test, null-hypothesis, slope = 0).

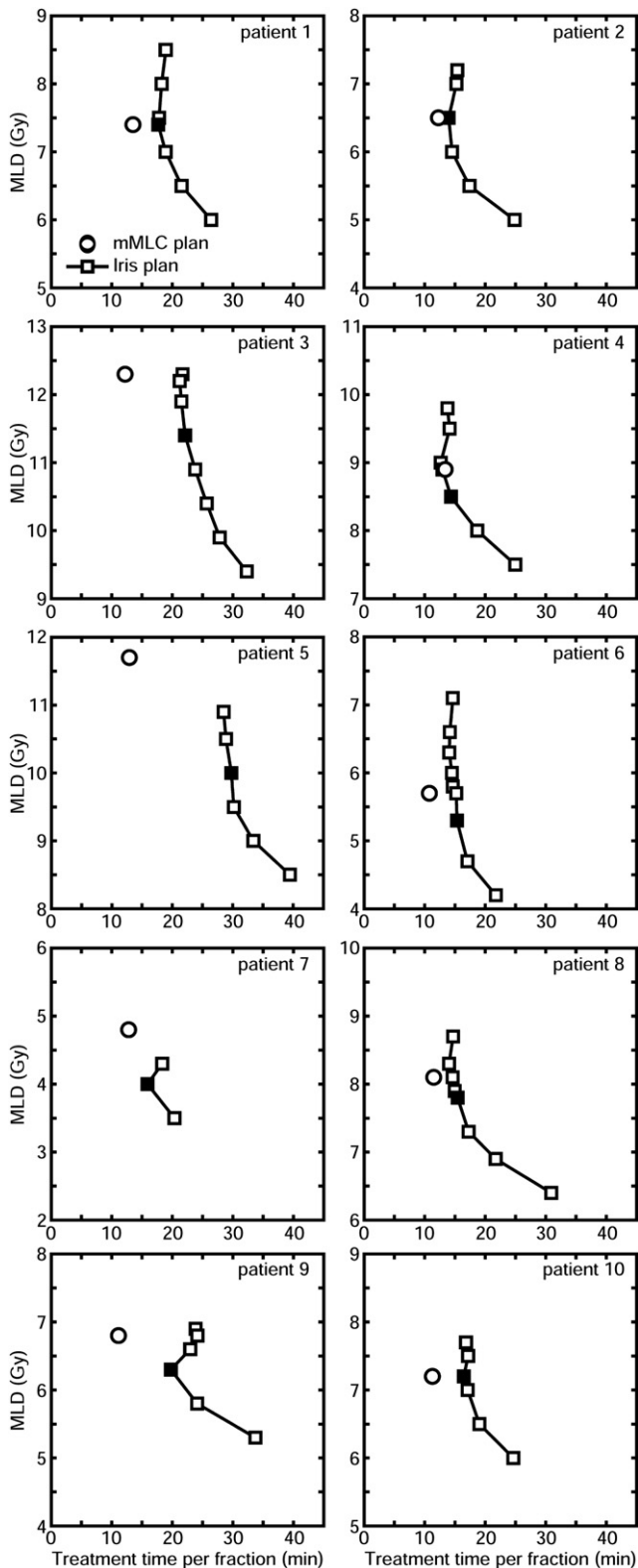


Fig. 4. Mean lung dose (MLD) as function of estimated fraction duration of mini-multileaf collimator plan and Iris plans. Each marker represents single treatment plan. Solid black markers indicate preferred Iris plans selected by physician.

from those using the MLD; sometimes, the same plan was selected as being equivalent. The preferred Iris plans selected by the physician had a lower MLD than the

MLD-equivalent Iris plans, and a treatment time/fraction of 18.1 min on average.

During Iris plan generation, the inverse planning algorithm performed an average of 7 resampling runs, thereby increasing the total number of candidate beams from 3,300 to 31,000 on average. The number of MUs was consequently reduced by an average of 28% compared with treatment planning without resampling. The beam reduction resulted, on average, in the use of 42% fewer beams at the cost of an increase in the number of MUs of only 5%. In 2 patients, the tumor was located within 2 cm of the spinal cord. The conformality constraint was sacrificed in the mMLC plans of these 2 patients to improve the sparing of the spinal cord. Moreover, The spinal cord constraint was relaxed to 8 Gy/fraction in one of these patients. The rib constraint was relaxed in the mMLC and Iris plans of 3 patients who had one or two ribs located partially within the PTV, because the PTV coverage was given the greatest priority. The dose distributions of the mMLC plan and MLD-equivalent Iris plan of Patient 4 are given in Fig. 2.

The variation in the fraction durations of the mMLC plans was small, but they varied greatly for the Iris plans (Fig. 3). Figure 3 shows that the fraction duration increased with an increasing target volume when using circular fields, similar for MLD-equivalent Iris plans ($p = .007$) and CI-equivalent Iris plans ($p < .001$). When conformally shaped fields were applied, the treatment time for each fraction was not significantly influenced by the target volume ($p = .6$). Thus, the fraction duration of MLD-equivalent plans was, on average, 40% longer than that of the mMLC plans for tumors $<80 \text{ cm}^3$ and $\leq 121\%$ longer for larger targets. For 1 patient, the Iris plan (same plan as for the MLD-equivalent and CI-equivalent plans) was more time-efficient than the mMLC plan. For this patient, this could be explained by the fact

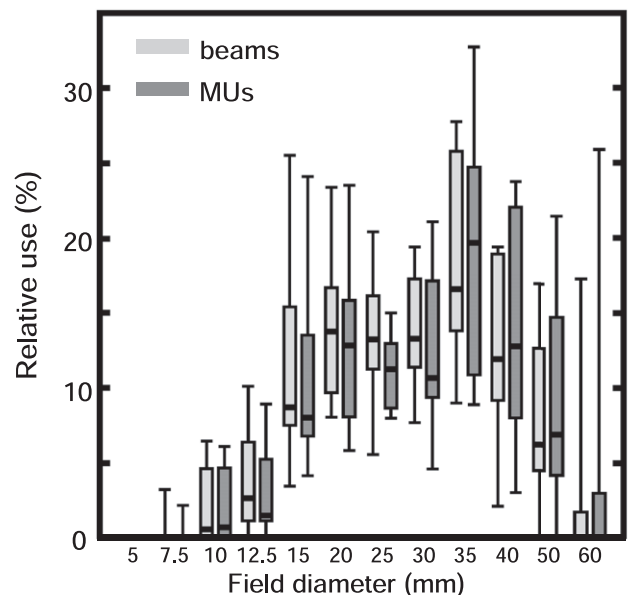


Fig. 5. Box plots of relative use of field sizes in mean lung dose-equivalent Iris plans of all patients, measured in number of beams and monitor units delivered. Whiskers indicate extreme values.

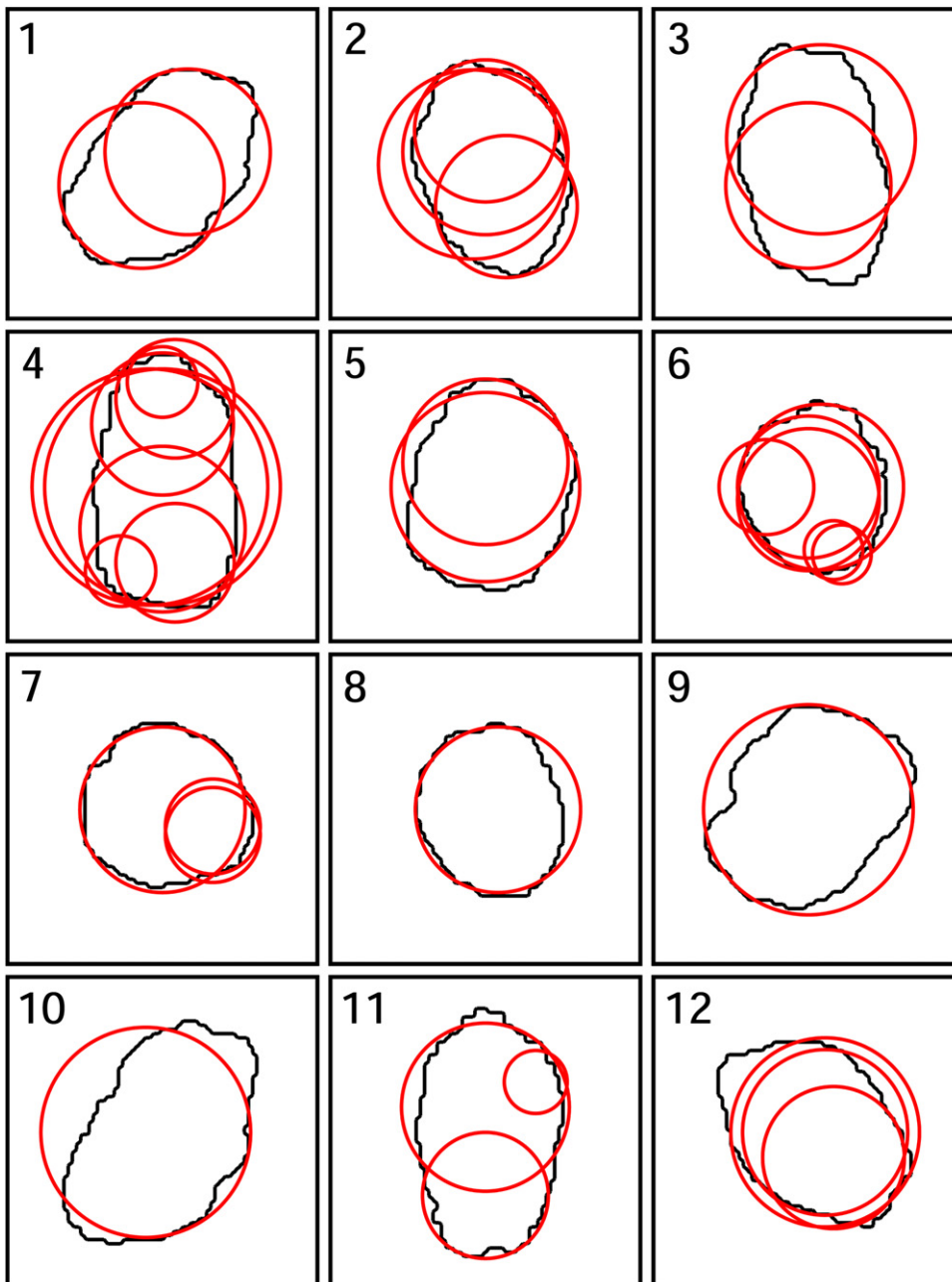


Fig. 6. Targeting of beams from node positions in mean lung dose-equivalent Iris plan of Patient 4. For each node position, beam's eye view projection of planning target volume given in black, and field contour (50% isodose) of each beam in red.

that the Iris plan contained only 12 of the 16 node positions of the mMLC plan. Although Iris plan generation started with all the node positions of the mMLC plan, some node positions were not selected by the inverse optimization algorithm. This was also observed in 5 other patients, but to a much lesser extent.

In Fig. 4, the MLD is plotted as a function of the estimated fraction duration for the mMLC plan (with a minimized MLD) and all Iris plans (with various MLD constraints) of each patient. The solutions in the lower part of each Iris graph are Pareto-efficient in terms of the MLD and fraction duration. Thus, a reduction in MLD was inevitably accompanied by an increase in the fraction duration and vice versa.

However, this Pareto-efficiency no longer holds for a greater MLD, because the solutions are restricted by different constraints in both regions of the graphs. The prescribed MLD is the limiting constraint in the lower part of the graphs, and the CI constraint is limiting in the upper part. The CI constraint also restricts the maximal MLD that can be obtained, which, in 2 patients, was even lower than the minimized MLD of the mMLC plan. The lowest MLD in all patients was obtained using the Iris collimator.

On average, nine collimator sizes were used in the MLD-equivalent Iris plans. Figure 5 shows the relative use of the collimator sizes, measured in the number of beams and in the number of MUs delivered. The smallest collimator size

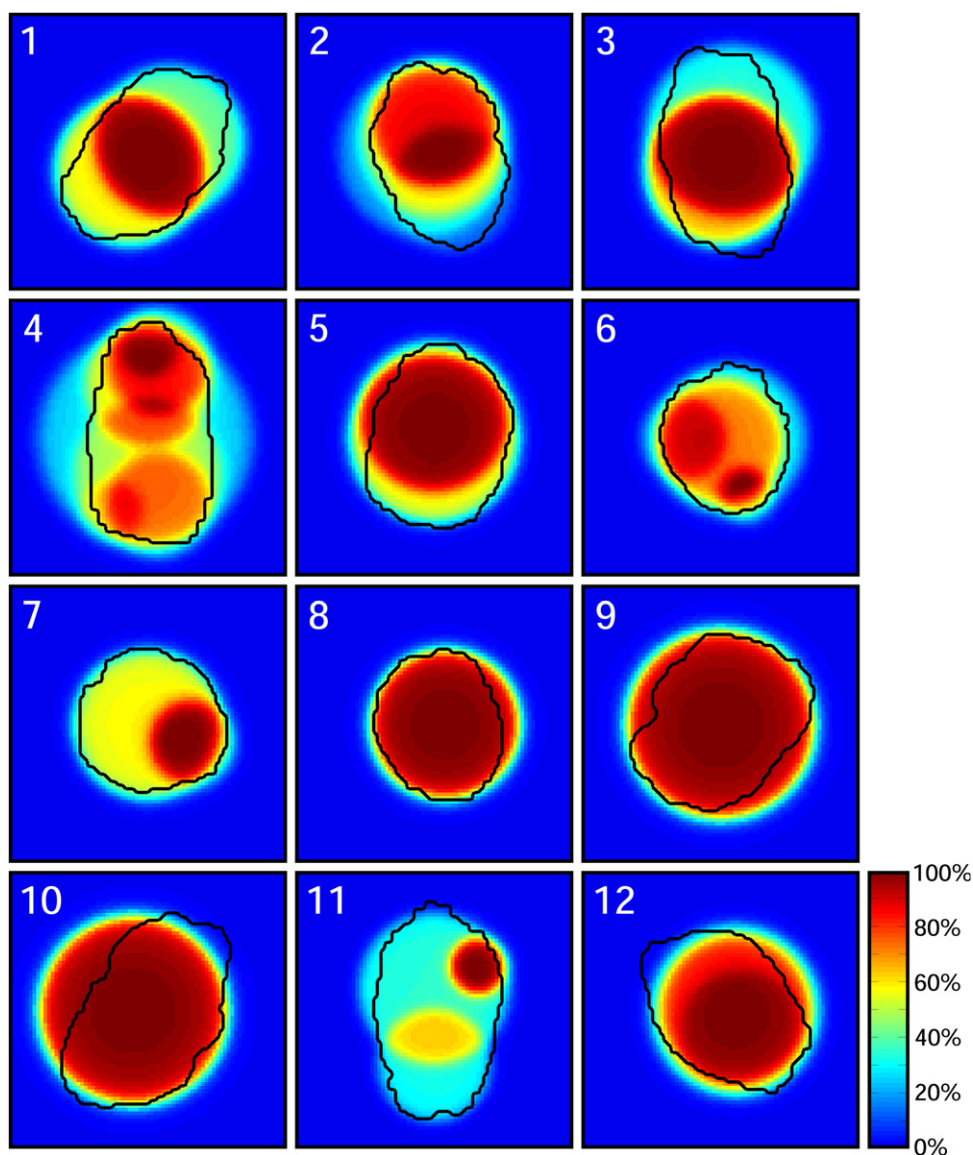


Fig. 7. Delivered fluence corresponding to Fig. 6. Beam's eye view projection of planning target volume given in black. Fluences normalized to maximal fluence for each node position.

was never used, while beams with field diameters of 15–40 mm were present in every treatment plan. A collimator size of 35 mm was, on average, most frequently used. The four largest collimator sizes delivered more MU/beam than the smaller collimators. Figure 6 shows the targeting of beams in the MLD-equivalent Iris plan of Patient 4. The large fields were typically aimed at the center of the PTV, and the smaller beams were used to deliver the dose at the PTV periphery. The corresponding fluence profiles of each node position are given in Fig. 7. Considerable fluence variation (*i.e.*, intensity modulation) was observed within almost all fields delivered from each node position.

DISCUSSION

The use of a mMLC on the CyberKnife was found to give time-efficient treatment plans in lung cancer patients. Iris plans generally had a greater treatment time/fraction, espe-

cially in large tumor volumes. Both the mMLC and Iris plans were much more time-efficient than the traditional fixed-collimator plans, which contain, for these patients, approximately 60 nodes positions, 125 beams, and 35,000 MUs. The Iris plans are also likely to be more time-efficient than the two-collimator plans from the study by Pöll *et al.* (1) for the same patient group. The Iris plans contained an average of 47% fewer beams and 2% more MUs. Although the number of node positions in the two-collimator plans was not reported, it is evidently expected to be much greater than in the Iris plans. The average MLD and CI were also considerably lower in the Iris plans.

The mMLC plans and Iris plans were generated using two different planning algorithms. Therefore, our observations could be biased by differences in these algorithms. As both algorithms were developed in-house, the parts of the algorithms such as structure segmentation, heterogeneity correction, dose grids, and plan evaluation, were deliberately

kept similar. However, some differences were inevitable, because the algorithms had to serve a different purpose (beam-angle optimization vs. inverse optimization for given node positions) and had to manage different field characteristics (isocentric conformal uniform beams vs. nonisocentric circular nonuniform beams). Another limitation of the present study was that a CyberKnife equipped with a mMLC and a flattening filter does not exist. The beam model, derived from a 6-MV gantry-based stereotactic linear accelerator, could therefore not be verified with a real machine. We furthermore assumed the use of an idealized mMLC. Instead of performing actual leaf segmentation, an arbitrarily orientated collimator grid was used with 2.5-mm resolution. Moreover, the mMLC was assumed to perfectly block the beam.

In the present study, we used flattened fields for the mMLC plans. Unflattened fields are becoming more common but require intensity modulation to cope with the nonuniform beam profiles, especially for larger tumors. The use of intensity-modulated radiotherapy (IMRT) on conventional gantries caused the delivery time to increase considerably compared with that for 3D-CRT. Because the aim of the present study was to improve the time efficiency of the CyberKnife treatments, we benchmarked the Iris plans with flattened nonintensity-modulated fields. To account for a flattening filter, the beam-on time was increased by 20%. The estimated mMLC fraction duration was, however, rather insensitive to this assumption. If a dose rate loss of 30% was assumed instead, the average mMLC treatment time would increase by only 4%. The use of flattened and unflattened fields in relation to plan quality and treatment time is the subject of future research.

The mMLC plans were not reproduced exactly by the Iris plans. This was, for example, illustrated by the dose distributions in Fig. 2 and by the fact that not all node positions of the mMLC plans were selected in the Iris plans. Moreover, Fig. 7 shows that the fluence profiles were highly modulated in the Iris plans. In contrast, a uniform fluence was used in the mMLC plans. Thus, the dosimetric plan quality of the Iris plans could be superior to that of the mMLC plans. However, it raises the question of whether the node positions selected by Cycle were optimal for use in the Iris plans. de Pooter *et al.* (4) used a similar approach for liver tumors, in which the selection of beam orientations by Cycle was followed by inverse IMRT optimization. The two-step optimization of beam orientations and IMRT profiles was, in some cases, found to result in suboptimal treatment plans. It is, therefore, likely that the quality of the Iris plans can be improved further if the beam orientation selection is integrated into the inverse planning algorithm. Simultaneous orientation and profile optimization for IMRT and CyberKnife are currently being developed at our institute.

CONCLUSION

Noncoplanar robotic stereotactic radiotherapy using a mMLC was found to give very time-efficient treatment plans in lung cancer patients. For small target volumes ($<80 \text{ cm}^3$), the Iris variable-aperture collimator is a time-efficient alternative to a mMLC. The fraction duration of these Iris plans (MLD-equivalent) was, on average, 40% longer than mMLC plans, with similar or better plan quality. For larger tumors, the treatment time of the Iris plans was $\leq 121\%$ longer.

REFERENCES

- Pöll JJ, Hoogeman MS, Prévost J, *et al.* Reducing monitor units for robotic radiosurgery by optimized use of multiple collimators. *Med Phys* 2008;35:2294–2299.
- Echner GG, Kilby W, Lee M, *et al.* The design, physical properties and clinical utility of an iris collimator for robotic radiosurgery. *Phys Med Biol* 2009;54:5359–5380.
- Liu R, Buatti JM, Howes TL, *et al.* Optimal number of beams for stereotactic body radiotherapy of lung and liver lesions. *Int J Radiat Oncol Biol Phys* 2006;66:906–912.
- de Pooter JA, Romero AM, Wunderink W, *et al.* Automated non-coplanar beam direction optimization improves IMRT in SBRT of liver metastasis. *Radiother Oncol* 2008;88:376–381.
- Hoogeman M, Prévost J, Nuyttens J, *et al.* Clinical accuracy of the respiratory tumor tracking system of the CyberKnife: Assessment by analysis of log files. *Int J Radiat Oncol Biol Phys* 2009;74:297–303.
- Timmerman R, Galvin J, Michalski J, *et al.* Accreditation and quality assurance for Radiation Therapy Oncology Group: Multicenter clinical trials using stereotactic body radiation therapy in lung cancer. *Acta Oncol* 2006;45:779–786.
- Woudstra E, Heijmen BJM, Storchi PRM. A comparison of an algorithm for automated sequential beam orientation selection (Cycle) with simulated annealing. *Phys Med Biol* 2008;53:2003–2018.
- de Pooter JA, Méndez Romero A, Jansen WPA, *et al.* Computer optimization of noncoplanar beam setups improves stereotactic treatment of liver tumors. *Int J Radiat Oncol Biol Phys* 2006;66:913–922.
- Breedveld S, Storchi PRM, Heijmen BJM. The equivalence of multi-criteria methods for radiotherapy plan optimization. *Phys Med Biol* 2009;54:7199–7209.
- Schweikard A, Schlaefer A, Adler JR. Resampling: An optimization method for inverse planning in robotic radiosurgery. *Med Phys* 2006;33:4005–4011.
- Borst GR, Ishikawa M, Nijkamp J, *et al.* Radiation pneumonitis after hypofractionated radiotherapy: Evaluation of the LQ(L) model and different dose parameters. *Int J Radiat Oncol Biol Phys* 2010;77:1596–1603.